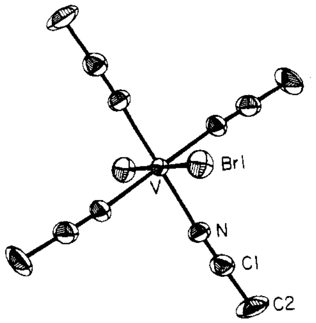

Figure 1. ORTEP view of $[VBr_2(CH_3CN)_4]^+$, at the 50% probability level.

Table III. Bond Distances (Å) and Angles (deg) in $[VBr_2(CH_3CN)_4]Br_3$

	Distances		
Br(1)–V	2.435 (1)	C(1)–C(2)	1.452 (9)
V–N	2.087 (4)	Br(2)–Br(3)	2.548 (1)
N–C(1)	1.126 (7)		
	Angles		
Br(1)–V–N	90.30 (9)	V–N–C(1)	176.0 (4)
N–V–N′	89.0 (2)	N–C(1)–C(2)	179.2 (6)

Table IV. Structure of the Tribromide Ion As Found Crystallographically in Six Compounds

compd	Br′–Br–Br″, deg	Br–Br′, Å	Br–Br″, Å	Br′···Br″, Å	ref
$[VBr_2(CH_3CN)_4]Br_3$	180[a]	2.548 (1)	2.548 (1)	5.096 (2)	*b*
$[(C_6H_5)_4P]Br_3$	177.62 (2)	2.5505 (4)	2.5505 (4)	5.1010 (6)	*c*
$[S_4N_3]Br_3$	179 (1)	2.677 (2)	2.431 (2)	5.108 (3)	*d*
$CsBr_3$	177.5 (5)	2.698 (6)	2.440 (6)	5.138 (9)	*e*
$[CS_3N_2Br]Br_3$	178.8 (1)	2.721 (1)	2.417 (2)	5.138 (2)	*f*
$[PBr_4]Br_3$	177 (1)	2.91 (1)	2.39 (1)	5.30 (2)	*g*

[a] Figure without esd implies an exact value required by symmetry. [b] This work. [c] Bogaard, M. P.; Rae, A. D. *Cryst. Struct. Commun.* **1982**, *11*, 175. [d] Mayerle, J. J.; Wolmershauser, G.; Street, G. B. *Inorg. Chem.* **1979**, *18*, 1161. [e] Breneman, G. L.; Willett, R. D. *Acta Crystallogr., Sect. B: Struct. Crystallogr. Cryst. Chem.* **1969**, *B25*, 1073. [f] Wolmershauser, G.; Krüger, C.; Tsay, Y.-H. *Chem. Ber.* **1982**, *115*, 1126. [g] Breneman, G. L.; Willett, R. D. *Acta Crystallogr.* **1967**, *23*, 467.

times its estimated standard deviation. The refinement gave residuals (defined and summarized in Table I) of $R = 0.031$ and $R_w = 0.042$ and goodness-of-fit = 0.994. A final difference Fourier map following refinement exhibited random peaks as high as 0.51 e/Å^3. The positional parameters are listed in Table II.

Results and Discussion

The structure of the compound, *trans*-$[VBr_2(CH_3CN)_4]Br_3$, is presented in Figure 1, and the important dimensions are listed in Table III. Both the cation and the Br_3^- ion have crystallographic C_{2h} $(2/m)$ symmetry. The cation has very nearly D_{4h} symmetry, except for very slight deviations of the N–V–N, V–N–C, and N–C–C angles from 90, 180, and 180°, respectively.

The Br_3^- Ion. Although this ion is much less stable or common than its congener I_3^- and does not, for example, exist in aqueous solution, it has been structurally characterized in several crystalline compounds (Table IV). In the present compound we have the only reported case of a completely symmetrical Br_3^- ion, i.e., one that both is rigorously linear and has identical Br–Br distances. There was one reported earlier that resides on a crystallographic twofold axis and thus has equal bond lengths but deviates slightly from linearity. All of the others show significantly disparate bond lengths, although they deviate but little from linearity. It is notable that the greater the disparity in the bond lengths, the greater their sum.

The compound we have prepared and studied is not new. It was reported in 1965 by Hathaway and Holah,[3] who correctly deduced its constitution from a combination of its elemental analysis, visible spectrum, IR spectrum, and magnetic moment. Our X-ray work fully confirms their proposal. It is to be noted that, in Hathaway and Holah's work, vanadium metal reacted directed with a solution of bromine in acetonitrile, without the application of a potential. We have also found this to be true. The same product, $[VBr_2(CH_3CN)_4]Br_3$, was obtained by us whether a voltage was applied or not.

In view of our experience, we were puzzled by the earlier claim[2] that $VBr_2{\cdot}CH_3CN$ could be obtained under similar conditions. We therefore corresponded with Professor D. G. Tuck, who carried out an electrochemical reaction to produce a sample of what was presumed to be $VBr_2{\cdot}CH_3CN$. We examined this material crystallographically and found that it was $[VBr_2(CH_3CN)_4]Br_3$. It is to be noted that analysis for the element bromine, though simple to do, is essentially useless for distinguishing between the two formulas since the bromine percentages are 63.9% for $VBr_2{\cdot}CH_3CN$ and 65.0% for $[VBr_2(CH_3CN)_4]Br_3$. Professor D. G. Tuck has reinvestigated the preparative procedure and has found that in his laboratory the product now obtained is also $VBr_5{\cdot}4CH_3CN$; he has requested us to make it clear that there is now no disagreement between our two laboratories.

Acknowledgment. We thank the Robert A. Welch Foundation for support under Grant No. A-494 and Professor D. G. Tuck for his helpful comments and for supplying a sample.

Registry No. $[VBr_2(CH_3CN)_4]Br_3$, 103664-47-7; $VBr_2{\cdot}CH_3CN$, 64345-05-7.

Supplementary Material Available: A table of anisotropic displacement parameters (1 page); a listing of structure factors (4 pages). Ordering information is given on any current masthead page.

---

(3) Hathaway, B. J.; Holah, D. G. *J. Chem. Soc.* **1965**, 537.

Contribution from the Department of Chemistry
and Laboratory for Molecular Structure and Bonding,
Texas A&M University, College Station, Texas 77843,
and Department of Chemistry, The Technion-Israel
Institute of Technology, Haifa, Israel

Derivatization of the Cuboidal Mo_4S_4–Aquo Ion: Preparation and Structure of $Mo_4S_4(HB(pz)_3)_4(pz)$ (pz = Pyrazolyl, $C_3N_2H_3^-$)

F. Albert Cotton,*[†] Zvi Dori,*[†‡] Rosa Llusar,[†]
and Willi Schwotzer[†]

Received February 12, 1986

The deliberate assembly of metal cluster compounds, starting from the composition of the core and extending to the choice of the ligand sphere, represents a synthetic challenge. Our own approach to the preparation of tri- and tetranuclear clusters of molybdenum and tungsten has in the past involved aqueous routes, because the aqueous chemistry of these elements is dominated by the presence of polynuclear species, many of them with M–M bonds.[1] These aquo species are attractive synthons since they are in essence composed of the cluster core surrounded by kinetically fairly labile water ligands.

Recently the cuboidal cluster aquo ion $[Mo_4S_4]_{aquo}$ has been prepared by Sykes[2] as well as by us[3] by different synthetic routes. In this paper we report the preparation of a derivative, $Mo_4S_4(HB(pz)_3]_4(\mu\text{-pz})$ (pz = pyrazolyl, $C_3N_2H_3^-$). The molecular compound is soluble in organic solvents, which demonstrates that the concept of cluster synthesis by aquo species does not restrict

---

[†] Texas A&M University.
[‡] The Technion-Israel Institute of Technology.

0020-1669/86/1325-3529$01.50/0 © 1986 American Chemical Society

Table I. Crystal Data for $Mo_4S_4(HB(pz)_3)_4(pz)$

formula	$Mo_4S_4B_4N_{26}C_{39}H_{43}$
fw	1431.2
space group	$C2/c$
syst absences	hkl, $h + k = 2n$; $h0l$, $h, l = 2n$
a, Å	19.067 (4)
b, Å	20.789 (2)
c, Å	18.145 (3)
β, deg	121.64 (2)
V, Å^3	6123 (4)
Z	4
d_{calcd}, g/cm^3	1.55
cryst size, mm	0.1 × 0.1 × 0.05
μ(Mo Kα), cm^{-1}	9.63
data collcn instrum	Enraf-Nonius CAD-4
radiation (monochromated in incident beam)	Mo Kα ($\lambda\bar{\alpha}$ = 0.71073 Å)
orientation reflcns: number, range (2θ)	25, 10–25
temp, °C	25
scan method	ω–2θ
data collcn range 2θ, deg	4–42
no. of unique data; total with $F_o^2 > 3\sigma(F_o^2)$	2699; 1375
no. of params refined	175
R,[a] %	6.69
R_w,[b] %	7.99
quality-of-fit indicator[c]	1.67
largest shift/esd, final cycle	0.21
largest peak, e/Å^3	1.5

[a] $R = \sum||F_o| - |F_c||/\sum|F_o|$. [b] $R_w = [\sum w(|F_o| - |F_c|)^2/\sum w|F_o|^2]^{1/2}$; $w = 1/\sigma^2(|F_o|)$. [c] Quality-of-fit $= [\sum w(|F_o| - |F_c|)^2/(N_{observns} - N_{params})]^{1/2}$.

this chemistry to aqueous media.

Experimental Section

A solution of the Mo_4S_4 aquo ion was prepared as previously described[3] except for the following modification: the ratio of $Mo(CO)_6$ to Na_2S was increased to 1:4. This improved the yield of the tetranuclear species and reduced the amount of the Mo_3S_4 trimer aquo ion.[1a] The eluate from the cation exchanger containing the Mo_4S_4 aquo ion was vacuum-dried to yield a green powder. The concentration of aqueous solutions prepared from this powder was established from UV absorption.

Preparation of $Mo_4S_4(HB(pz)_3)_4$ (pz) (1). Addition of a 10 molar excess of $KHB(pz)_3$ to 20 mL of a 6×10^{-3} M solution of the aquo ion resulted in an almost instantaneous color change to brown and the deposition of an amorphous precipitate. It was stirred for 24 h. Addition of CH_2Cl_2 then resulted in the extraction of the title compound into the organic layer. The red-brown CH_2Cl_2 phase was separated and dried. The title compound was isolated by fractional precipitation with hexane. Yield: 80%.

X-ray Crystallography. Growth of crystals suitable for diffraction work was attempted by a variety of conventional methods such as layering, slow cooling of various solvent mixtures, etc. Well-shaped though very small crystals were finally obtained by slow diffusion of hexane into a CH_2Cl_2 solution.

A red-brown rhomboidal plate of dimensions 0.1 × 0.1 × 0.05 mm was sealed inside a Lindemann capillary. Data were collected on an automated four-circle diffractometer. Three reflections monitored throughout the data collection displayed no significant change in intensity. Many data pertaining to data collection and refinement are in Table I.[4] The positions of the two independent Mo and S atoms were obtained by direct methods (MULTAN), and the remainder of the atoms were located and refined by alternating difference Fourier and least-squares methods. Anisotropic displacement parameters were introduced only for the Mo and S atoms in order to maintain a satisfactory data-to-parameter ratio. Convergence was reached at residuals of R = 7.7% and R_w = 8.8% with a goodness-of-fit parameter of 2.1. A cluster of electron density peaks, unrelated to the main molecule and with intensities up to 1.5 e/Å^3, remained in the last Fourier map. Although no simple model could be fit to those peaks, distances and angles were indicative of disordered hexane. We then decided to include in the refinement a "hexane-type" chain of carbon atoms, with half-occupancy and fixed thermal parameters and positions. This reduced the residuals to R = 6.69% and R_w = 7.99% and, more importantly, the goodness-of-fit to 1.67. Fractional coordinates are listed in Table II.

Table II. Atomic Positional Parameters and Equivalent Isotropic Displacement Parameters (Å^2) and Their Estimated Standard Deviations for $Mo_4S_4(HB(pz)_3)_4(pz)$

atom	x	y	z	B
Mo1	0.4374 (1)	0.3978 (1)	0.1585 (1)	2.36 (5)
Mo2	0.4399 (1)	0.2932 (1)	0.2666 (1)	2.47 (5)
S1	0.4167 (3)	0.4059 (3)	0.2747 (3)	2.4 (2)
S2	0.4203 (3)	0.2894 (4)	0.1277 (3)	2.4 (2)
N1	0.440 (1)	0.416 (1)	0.041 (1)	3.0 (5)*
N2	0.386 (1)	0.456 (1)	–0.025 (1)	3.2 (5)*
N3	0.406 (1)	0.507 (1)	0.144 (1)	3.2 (5)*
N4	0.361 (1)	0.532 (1)	0.063 (1)	4.7 (6)*
N5	0.302 (1)	0.401 (1)	0.066 (1)	4.3 (5)*
N6	0.266 (1)	0.442 (1)	–0.009 (1)	4.2 (6)*
N7	0.425 (1)	0.2632 (9)	0.375 (1)	2.3 (5)*
N8	0.358 (1)	0.274 (1)	0.383 (1)	3.9 (6)*
N9	0.311 (1)	0.2586 (9)	0.197 (1)	2.3 (5)*
N10	0.253 (1)	0.271 (1)	0.223 (1)	3.8 (6)*
N/C11	0.172 (2)	0.367 (2)	0.318 (2)	7.9 (9)*
N12	0.210 (1)	0.309 (1)	0.322 (1)	5.2 (6)*
N13	0.469 (1)	0.192 (1)	0.261 (1)	3.9 (5)*
C1	0.496 (1)	0.397 (1)	0.019 (1)	3.3 (6)*
C2	0.472 (1)	0.417 (1)	–0.065 (1)	2.9 (6)*
C3	0.408 (1)	0.456 (1)	–0.087 (1)	3.4 (6)*
C4	0.407 (1)	0.549 (1)	0.199 (1)	3.2 (6)*
C5	0.365 (1)	0.605 (2)	0.153 (1)	4.8 (7)*
C6	0.337 (1)	0.591 (2)	0.072 (2)	5.3 (8)*
C7	0.237 (2)	0.374 (1)	0.067 (2)	5.4 (8)*
C8	0.163 (1)	0.391 (2)	–0.009 (2)	5.0 (8)*
C9	0.181 (1)	0.434 (1)	–0.050 (2)	4.5 (7)*
C10	0.479 (1)	0.230 (1)	0.445 (2)	4.6 (8)*
C11	0.445 (2)	0.217 (2)	0.498 (2)	5.9 (8)*
C12	0.365 (2)	0.245 (2)	0.456 (2)	7 (1)*
C13	0.271 (1)	0.220 (1)	0.128 (1)	4.0 (7)*
C14	0.193 (1)	0.206 (1)	0.110 (1)	3.9 (6)*
C15	0.184 (1)	0.235 (1)	0.170 (2)	4.0 (7)*
C16	0.106 (2)	0.343 (2)	0.335 (2)	9 (1)*
C17	0.111 (2)	0.273 (2)	0.344 (2)	7 (1)*
N/C18	0.175 (1)	0.255 (1)	0.337 (1)	5.2 (7)*
C19	0.454 (2)	0.132 (2)	0.263 (2)	5.9 (8)*
C20	0.500	0.089 (2)	0.250	6 (1)*
B1	0.319 (2)	0.492 (2)	–0.017 (2)	4.5 (9)*
B2	0.285 (2)	0.314 (2)	0.310 (2)	3.6 (8)*
C25S	0.6992	–0.9707	0.7011	8*
C26S	0.2988	0.0156	0.2988	8*
C24S	0.3828	0.0000	0.3496	8*
C28S	0.2324	0.4316	0.7148	8*
C23S	0.4160	0.0488	0.4316	8*
C22S	0.4316	0.0156	0.4824	8*

[a] Values marked with an asterisk indicate that the atoms were refined isotropically. Anisotropically refined atoms are given in the form of the equivalent isotropic displacement parameter defined as $^4/_3[a^2\beta_{11} + b^2\beta_{22} + c^2\beta_{33} + ab(\cos\gamma)\beta_{12} + ac(\cos\beta)\beta_{13} + bc(\cos\alpha)\beta_{23}]$.

Results and Discussion

Structure and Bonding. $Mo_4S_4(HB(pz)_3)_4(pz)$ (1) is a molecular compound. An ORTEP drawing that also defines the atom-num-

---

(1) (a) Bino, A.; Cotton, F. A.; Dori, Z. *J. Am. Chem. Soc.* **1978**, *100*, 5252. (b) Bino, A.; Cotton, F. A.; Dori, Z. *J. Am. Chem. Soc.* **1979**, *101*, 3842. (c) Cotton, F. A.; Marler, D. O.; Schwotzer, W. *Inorg. Chem.* **1984**, *23*, 3671. (d) Dori, Z.; Cotton, F. A.; Llusar, R.; Schwotzer, W. *Polyhedron* **1986**, *5*, 907. (e) Cotton, F. A.; Dori, Z.; Llusar, R.; Schwotzer, W. *J. Am. Chem. Soc.* **1985**, *107*, 6734. (f) Richens, D. T.; Sykes, A. g. *Comments Inorg. Chem.* **1981**, *1*, 151.

(2) Kathirgamanthan, P.; Martinez, M.; Sykes, A. G. *J. Chem. Soc., Chem. Commun.* **1985**, 953.

(3) Cotton, F. A.; Diebold, M. P.; Dori, Z.; Llusar, R.; Schwotzer, W. *J. Am. Chem. Soc.* **1985**, *107*, 6735.

(4) The Enraf-Nonius Structure Determination Package (SDP Plus) was used for all crystallographic computations.

(5) Müller, A.; Eltzner, W.; Bögge, H.; Jostes, R. *Angew. Chem., Int. Ed. Engl.* **1982**, *21*, 795.

(6) Bandy, J. A.; Davies, C. E.; Green, J. V. C.; Green, M. L. H.; Prout, K.; Rogers, D. P. S. *J. Chem. Soc., Chem. Commun.* **1983**, 1395.

(7) Shibahara, T.; Kuroya, H.; Matsumoto, K.; Ooi, S. *Inorg. Chim. Acta* **1986**, *116*, L25.

(8) Shibahara, T.; Kuroya, H.; Matsumoto, K.; Ooi, S. *J. Am. Chem. Soc.* **1984**, *106*, 789.

(9) Mak, T. C. W.; Jasim, K. S.; Chieh, C. *Inorg. Chem.* **1985**, *24*, 1587.

Table III. Bond Distances and Angles within the Mo_4S_4 Core[a]

(a) Bond Distances (Å)

Mo1	Mo1′	2.899 (2)	Mo1	N1	2.19 (2)	Mo2	S2′	2.330 (5)
Mo1	Mo2	2.912 (4)	Mo1	N3	2.34 (2)	Mo2	N7	2.22 (2)
Mo1	Mo2′	2.952 (3)	Mo1	N5	2.23 (2)	Mo2	N9	2.22 (2)
Mo1	S1	2.347 (8)	Mo2	Mo2′	2.659 (4)	Mo2	N13	2.20 (2)
Mo1	S1′	2.386 (6)	Mo2	S1	2.404 (8)			
Mo1	S2	2.304 (8)	Mo2	S2	2.346 (7)			

(b) Bond Angles (deg)

Mo1′	Mo1	Mo2	61.05 (8)	S1′	Mo1	S2	99.9 (2)	Mo2′	Mo2	S1	102.8 (2)
Mo1′	Mo1	Mo2′	59.69 (7)	S1′	Mo1	N1	82.5 (5)	Mo2′	Mo2	S2	55.1 (2)
Mo1′	Mo1	S1	52.9 (1)	S1′	Mo1	N3	98.5 (5)	Mo2′	Mo2	S2′	55.6 (2)
Mo1′	Mo1	S1′	51.6 (2)	S1′	Mo1	N5	164.7 (7)	Mo2′	Mo2	N7	136.5 (4)
Mo1′	Mo1	S2	101.8 (2)	S2	Mo1	N1	90.5 (6)	Mo2′	Mo2	N9	134.7 (6)
Mo1′	Mo1	N1	133.7 (4)	S2	Mo1	N3	158.7 (4)	Mo2′	Mo2	N13	73.7 (6)
Mo1′	Mo1	N3	98.0 (4)	S2	Mo1	N5	83.4 (7)	S1	Mo2	S2	99.7 (3)
Mo1′	Mo1	N5	142.6 (7)	N1	Mo1	N3	81.3 (8)	S1	Mo2	S2′	98.6 (2)
Mo2	Mo1	Mo2′	53.92 (8)	N1	Mo1	N5	82.6 (8)	S1	Mo2	N7	96.1 (5)
Mo2	Mo1	S1	53.1 (2)	N3	Mo1	N5	76.0 (8)	S1	Mo2	N9	99.6 (5)
Mo2	Mo1	S1′	96.2 (2)	Mo1	Mo2	Mo1′	59.25 (7)	S1	Mo2	N13	176.2 (5)
Mo2	Mo1	S2	51.9 (2)	Mo1	Mo2	Mo2′	63.80 (9)	S2	Mo2	S2′	110.6 (2)
Mo2	Mo1	N1	141.8 (6)	Mo1	Mo2	S1	51.3 (2)	S2	Mo2	N7	157.0 (5)
Mo2	Mo1	N3	136.1 (6)	Mo1	Mo2	S2	50.6 (2)	S2	Mo2	N9	82.8 (6)
Mo2	Mo1	N5	97.5 (7)	Mo1	Mo2	S2′	100.7 (2)	S2	Mo2	N13	79.5 (6)
Mo2′	Mo1	S1	96.1 (2)	Mo1	Mo2	N7	147.4 (5)	S2′	Mo2	N7	83.2 (4)
Mo2′	Mo1	S2	50.8 (1)	Mo1	Mo2	N9	103.8 (5)	S2′	Mo2	N9	155.1 (5)
Mo2′	Mo1	N1	99.4 (5)	Mo1	Mo2	N13	126.8 (6)	S2′	Mo2	N13	78.3 (4)
Mo2′	Mo1	N3	149.9 (4)	Mo1′	Mo2	Mo2′	62.28 (9)	N7	Mo2	N9	78.1 (6)
Mo2′	Mo1	N5	134.1 (7)	Mo1′	Mo2	S1	51.7 (1)	N7	Mo2	N13	85.8 (8)
S1	Mo1	S1′	103.9 (2)	Mo1′	Mo2	S2	99.2 (2)	N9	Mo2	N13	84.0 (7)
S1	Mo1	S2	102.6 (3)	Mo1′	Mo2	S2′	50.0 (2)	Mo1′	S1	Mo2	76.1 (2)
S1	Mo1	N1	164.0 (6)	Mo1′	Mo2	N7	103.6 (4)	Mo1	S2	Mo2	77.6 (2)
S1	Mo1	N3	83.2 (6)	Mo1′	Mo2	N9	151.3 (5)	Mo1	S2	Mo2′	79.1 (2)
S1	Mo1	N5	89.8 (7)	Mo1′	Mo2	N13	124.7 (4)	Mo2	S2	Mo2′	69.3 (2)

[a] Numbers in parentheses are estimated standard deviations in the least significant digits.

Table IV. Mo–Mo Bond Lengths in $[Mo_4S_4]^{4+}$ Cluster Compounds

compd	no. of core electrons	Mo–Mo bond lengths, Å	ref
$[Mo_4S_4(CN)_{12}]^{8-}$	12	2.855 (1) (2×), 2.853 (1) (4×)	5
$[Mo_4S_4(i\text{-PrCp})_4]$	12	2.912 (1) (2×), 2.892 (1), 2.902 (1) (2×), 2.905 (1)	6
$[Mo_4S_4(i\text{-PrCp})_4]^+$	11	2.893 (1), 2.887 (1), 2.860 (1), 2.900 (1), 2.901 (1), 2.923 (1)	6
$[Mo_4S_4(i\text{-PrCp})_4]^{2+}$	10	2.861 (1), 2.902 (1), 2.897 (1), 2.820 (1), 2.790 (1), 2.879 (1)	6
$[Mo_4S_4(edta)_2]^{4-}$	12	2.769 (2), 2.791 (1), 2.790 (1), 2.769 (2)	7
$[Mo_4S_4(edta)_2]^{3-}$	11	2.775 (2), 2.794 (2), 2.880 (2), 2.845 (2), 2.755 (2), 2.796 (2)	8
$[Mo_4S_4(edta)_2]^{2-}$	10	2.741 (1), 2.870 (1), 2.843 (1), 2.780 (1), 2.872 (1), 2.853 (1)	7
$[Mo_4S_4(NCS)_{12}]^{6-}$	10	2.791 (1) (3×), 2.869 (1) (3×)	3
$Mo_4S_4(dtc)_6$ (dtc = dithiocarbamate)	10	2.732 (5) (2×), 2.858 (5) (2×), 2.859 (8), 2.890 (7)	9
$Mo_4S_4(HB(pz)_3)_4(\mu\text{-pz})$	11	2.92 (3) (5×), 2.659 (4)	this work

bering scheme is shown in Figure 1. Important bond lengths and angles are given in Table III. The cluster core consists of a cuboidal arrangement of Mo and S atoms leaving three facial octahedral coordination sites (not counting the M–M interactions) for ligand bonding. On two molybdenum atoms (Mo1 and Mo1′) these are occupied by pyrazolylborate anions in the typical tridentate chelating fashion. On the remaining two molybdenum atoms (Mo2 and Mo2′) the $Hb(pz)_3$ ligands function only as bidentate ligands with one pyrazole ring dangling. The third coordination site on each of these atoms is occupied by a μ-pyrazolyl ligand bridging the Mo2–Mo2′ edge. The cluster has crystallographically imposed C_2 symmetry and thus 4 independent Mo–Mo distances. The virtual symmetry of the core, however, is C_{2v}. The Mo_4 tetrahedron is compressed along the pyrazolyl-bridged edge. The Mo–Mo bond lengths are 2.92 [3] Å for all but the bridged edge, which is 2.659 (4) Å.

An electron count shows that there is a total of 59 electrons in the cluster, 48 of which are involved in metal–ligand bonds. This leaves 11 electrons for M–M bonding. The average bond order is therefore 11/12; viz., the cluster is electron-deficient with respect to a full set of Mo–Mo single bonds. In an MO description of the Mo_4S_4 core of T_d symmetry, the HOMO is a fully occupied (6 e) t_2-type orbital. Reducing the occupancy in this orbital would be expected to give rise to a Jahn–Teller effect to split the threefold degeneracy. This has been observed in all electron-deficient Mo_4S_4 systems on record, as can be seen from the data in Table IV. The prediction of what type of distortion is to be expected cannot be made on the basis of qualitative arguments. There is no question that the C_{2v} distortion in our case completely splits the degeneracy of the HOMO, but the presence of the one bridging pyrazole makes it difficult to assess how much of the distortion arises from the Jahn–Teller effect. It is possible that a distortion caused by the μ-pz^- ligand completely preempts any Jahn–Teller effect. A study of the 12-electron anion, which will be attempted, might clarify this question. Other types of distortions have previously been observed for 11-electron systems, most predominantly of the D_{2d}-type.

Synthesis. The isolation of the cuboidal cluster compound **1** corroborates our view that the Mo_4S_4 aquo ion represents a generic form of the Mo/S cubane and permits an easy entry into the chemistry of these compounds. The aquated core is reasonably stable under various conditions. It can, for example, be handled in air for hours without any sign of decomposition.

Naturally there are side reactions to be taken into account, most prominently hydrolysis reactions of the reagents. The bridging pyrazolate is believed to originate from hydrolysis. Experiments to circumvent its formation in order to prepare the homoleptic $Mo_4S_4(HB(pz)_3)_4$ complex are in progress.

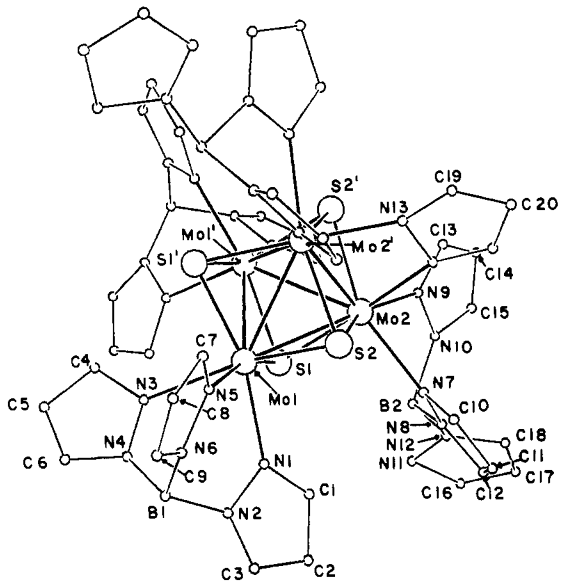

Figure 1. ORTEP drawing of $Mo_4S_4(HB(pz)_3)_4(pz)$ (**1**).

Finally, the oxidation state of the cluster deserves comment. We have previously[3] isolated a 10-electron cluster from the reaction of the aquo ion with NCS^-. The title compound, on the other hand, is an 11-electron cluster. Cyclic voltammetry on the Mo_4S_4 aquo species has revealed that the interconversions[2]

$$[Mo_4S_4]^{6+}\ (10\ e^-) \rightleftharpoons [Mo_4S_4]^{5+}\ (11\ e^-) \rightleftharpoons [Mo_4S_4]^{4+}\ (12\ e^-)$$

are facile. The E^0 values in 2 M *p*-toluenesulfonic acid are +0.54 and −0.08 V (vs. NHE) for the first and second steps, respectively. This clearly indicates that all three forms are accessible in aqueous medium and interconvertible by mild oxidants or reductants. It is therefore conceivable that $KHB(pz)_3$ is acting not only as a ligand but also as a reducing agent similar to $NaBH_4$, which was successfully employed in the reduction of $[Mo_4S_4(edta)_2]^{3-}$.

Acknowledgment. We thank the National Science Foundation for support.

Registry No. 1, 103619-49-4.

Supplementary Material Available: Tables of anisotropic displacement parameters and complete bond distances and angles (4 pages); a listing of structure factors (7 pages). Ordering information is given on any current masthead page.

Contribution from the Department of Chemistry,
University of Massachusetts, Amherst, Massachusetts 01003,
and Department of Molecular Spectroscopy,
Research Institute of Materials, University of Nijmegen,
Toernooiveld, 6525 ED Nijmegen, The Netherlands

Relation between Structure and Magnetic Exchange Pathways in Hexakis(pyridine *N*-oxide)copper Complexes

J. S. Wood[†] and C. P. Keijzers*[‡]

Received April 4, 1986

The hexakis(pyridine *N*-oxide) complexes $M(PyO)_6X_2$ ($M = Mn^{2+}$–Zn^{2+}; $X = ClO_4^-, BF_4^-, NO_3^-$) crystallize in space group $R\bar{3}$, with S_6 point symmetry for the octahedral complex ions. The anions have threefold symmetry.[1] The form of the antiferromagnetic exchange in the copper complexes is governed by the nature of the cooperative Jahn–Teller effect operative in the particular complex.[2] In the BF_4^- complex, the tetragonally elongated cations are ferrodistortively ordered at low temp.[3,4] and *two*-dimensional antiferromagnetism is found. In the ClO_4^- and NO_3^- complexes, the low-temperature ordering of the elongated octahedra is *anti*ferrodistortive[3,4] and *one*-dimensional antiferromagnetic behavior is found.[2] The two low-temperature structures are illustrated in Figure 1. The near equivalence (circa 1 K) of the intrachain exchange in the ClO_4^- complex and the intraplane exchange in the BF_4^- complex (which are defined as the *strong* exchange, J, in this note) suggests that the same superexchange pathway is operative in both complexes. This path has been assumed to result from a long-range interaction (overlap?) of the oxygen atoms of the PyO ligands of neighboring complexes.[2] However, the pathway might also involve the pyridine rings of the ligands since the lone pair density on the oxygen atom is directed toward the rings of neighboring molecules[5] and the oxygen–ring plane distance is only 3.28 Å at 20 K, while the O–O distance is 5.47 Å.[6] Since these initial results, EPR measurements on pairs of complexes[7,8] in heavily doped, diamagnetic, zinc host crystals gave important information on the small *inter*chain/plane exchange (defined as J') and they revealed that, for each anion, several different pair configurations are produced. The relative abundances of these pair configurations and also J' depend on

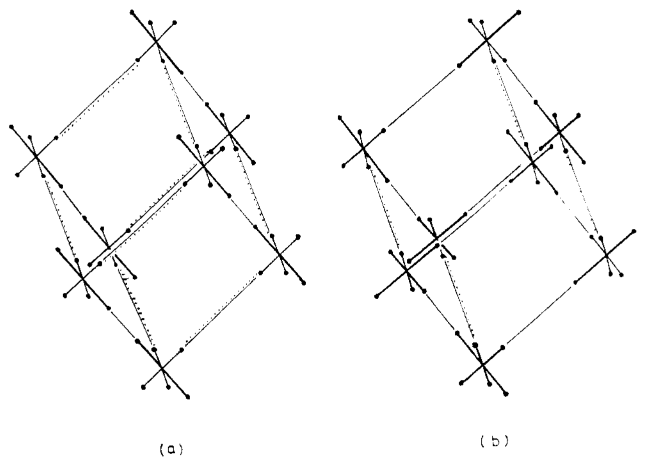

Figure 1. Rhombohedral unit cell of $Cu(PyO)_6^{2+}$ octahedra showing the low-temperature structures for (a) the ferrodistortive fluoborate complex and (b) the antiferrodistortive perchlorate and nitrate complexes. Dotted lines denote the directions of principal antiferromagnetic exchange.

Table I. Unit Cell Dimensions and Calculated Shortest Intermolecular O–O Distance in $M(PyO)_6X_2$ Complexes

	M = Cu			M = Zn		
X	*a*, Å	α, deg	O···O, Å	*a*, Å	α, deg	O···O, Å
ClO_4^-	9.620	81.21	5.600[a]	9.632	81.07	5.577[a]
	9.450	80.84	5.472[b]			
BF_4^-	9.621	81.46	5.592[a]	9.621	81.25	5.555[a]
NO_3^-	9.480	83.45	5.413[c]	9.503	83.38	*d*

[a] Reference 1c. [b] Results from neutron diffraction at 20 K, ref 6. [c] Reference 1d. [d] J. Smits, private communication.

[†] University of Massachusetts.

[‡] University of Nijmegen.

(1) (a) van Ingen Schenau, A. D.; Verschoor, G. C.; Romers, C. *Acta Crystallogr., Sect. B: Struct. Crystallogr. Cryst. Chem.* **1974**, *B30*, 1686. (b) Bergendahl, T. J.; Wood, J. S. *Inorg. Chem.* **1975**, *14*, 338. (c) O'Connor, C. J.; Sinn, E.; Carlin, R. L. *Inorg. Chem.* **1977**, *16*, 3314. (d) Wood, J. S.; Day, R. O. *Cryst. Struct. Commun.* **1981**, *10*, 255.

(2) Algra, H.; De Jongh, L.; Carlin, R. L. *Physica B+C* **1978**, *93*, 24.

(3) Reinen, D.; Krause, S. *Solid State Commun.* **1979**, *29*, 691.

(4) Wood, J. S.; Keijzers, C. P.; de Boer, E.; Buttafava, A. *Inorg. Chem.* **1980**, *19*, 2213.

(5) Wood, J. S. *Acta Crystallogr., Sect. A: Found. Crystallogr.* 1984, *A40*, C-166. Wood, J. S. to be submitted for publication.

(6) Keijzers, C. P.; McMullan, R. K.; Wood, J. S.; van Kalkeren, G.; Srinivasan, R.; de Boer, E. *Inorg. Chem.* **1982**, *21*, 4275.

(7) Van Kalkeren, G.; Keijzers, C. P.; Srinivasan, R.; de Boer, E.; Wood, J. S. *Mol. Phys.* **1983**, *48*, 1.

(8) Paulissen, M. L. H.; Keijzers, C. P. *J. Mol. Struct.* **1984**, *113*, 267.

0020-1669/86/1325-3532$01.50/0